



Research Paper

Quantitative analysis of morphological and functional features in Meibography for Meibomian Gland Dysfunction: Diagnosis and Grading

Yuqing Deng^{a,1}, Qian Wang^{a,1}, Zhongzhou Luo^a, Saiqun Li^a, Bowen Wang^a, Jing Zhong^a, Lulu Peng^a, Peng Xiao^{a,**}, Jin Yuan^{a,*}

^a State Key Laboratory of Ophthalmology, Zhongshan Ophthalmic Centre, Sun Yat-sen University, Guangzhou, Guangdong, China

ARTICLE INFO

Article History:

Received 8 June 2021

Revised 24 August 2021

Accepted 26 August 2021

Available online xxx

Keywords:

Meibography

Meibomian gland dysfunction

Automated meibomian glands analyser

ABSTRACT

Background: To explore the performance of quantitative morphological and functional analysis in meibography images by an automatic meibomian glands (MGs) analyser in diagnosis and grading Meibomian Gland Dysfunction (MGD).

Methods: A cross-sectional study collected 256 subjects with symptoms related to dry eye and 56 healthy volunteers who underwent complete ocular surface examination was conducted between January 1, 2019, and December 31, 2020. The 256 symptomatic subjects were classified into MGD group (n = 195) and symptomatic non-MGD group (n = 61). An automatic MGs analyser was used to obtain multi-parametric measurements in meibography images including the MGs area ratio (GA), MGs diameter deformation index (DI), MGs tortuosity index (TI), and MGs signal index (SI). Adjusted odds ratios (ORs) of the multi-parametric measurements of MGs for MGD, and the area under the receiver operating characteristic (AUC-ROC) curves of multi-parametric measurements for MGD diagnosing and grading were conducted.

Findings: When consider age, sex, ocular surface condition together, the estimated ORs for DI was 1.62 (95% CI, 1.29-2.56), low-level SI was 24.34 (95% CI, 2.73-217.3), TI was 0.76 (95% CI, 0.54-0.90), and GA was 0.86 (95% CI, 0.74-0.92) for MGD. The combination of DI-TI-GA-SI showed an AUC = 0.82 (P < 0.001) for discriminating MGD from symptomatic subjects. The DI had a higher AUC in identifying early-stage MGD (grade 1-2), while TI and GA had higher AUCs in moderate and advanced stages (grade 3-5). Merging DI-TI-GA showed the highest AUCs in distinguish MGD severities.

Interpretation: The MGs area ratio, diameter deformation, tortuosity and signal intensity could be considered promising biomarkers for MGD diagnosis and objective grading.

Funding: This work was supported by the Key-Area Research and Development Program of Guangdong Province (No. 2019B010152001), the National Natural Science Foundation of China under Grant (81901788) and Guangzhou Science and Technology Program (202002030412).

© 2021 The Authors. Published by Elsevier Ltd. This is an open access article under the CC BY-NC-ND license (<http://creativecommons.org/licenses/by-nc-nd/4.0/>)

1. Introduction

Meibomian Gland Dysfunction (MGD) is one of the most common ocular surface diseases extremely prevalent worldwide, especially in Asian populations (from 46.2% to 69.3%) [1,2]. As the most common trigger of dry eye diseases (DED) [2], MGD has also been reported to

be associated with lots of other ocular diseases, i.e., allergic conjunctivitis, ocular rosacea, Sjögren syndrome [3-5], and systemic factors such as androgen deficiency, dyslipidemia, and aging [6-8], that degrades patients' ocular comfort, visual function, and quality of life [9,10,11]. A high accuracy objective diagnosis strategy for MGD could provide significant benefits. However, existent diagnostic tests based on the observation of abnormal anatomy and physiology of the MGs opening and lid secretions [12] mostly rely on the experience of expert clinicians, making quantification difficult and more likely to be affected by interobserver variability. The variation of the results may also affect by involvement of gland selection errors, different pressure applied manually by the operators [13]. It's also difficult for some patients to cooperate with the squeeze examination with obvious inflammatory state of eye lids and too sensitive to invasive tests [10]. Moreover, DED and MGD have high similarities in symptoms

* **Correspondence Author:** Jin Yuan, MD, PhD Zhongshan Ophthalmic Centre, Sun Yat-Sen University, 7 Jinsui Road, Tianhe District, Guangzhou, China, 510060, Tel.: (86) 13825141659, Fax: (8620) 87331550

** **Correspondence Author:** Peng Xiao, PhD Zhongshan Ophthalmic Centre, Sun Yat-Sen University, 7 Jinsui Road, Tianhe District, Guangzhou, China, 510060, Tel.: (86) 18826070428, Fax: (8620) 87331550

E-mail addresses: xiaopengaddis@hotmail.com (P. Xiao), yuanjincornea@126.com (J. Yuan).

¹ These authors contributed equally to this manuscript.

Research in context

Evidence before this study

We searched PubMed for articles published between January 1, 2000 and May 1, 2021 using the terms: ("meibomian gland dysfunction" OR "meibomian" OR "meibography") AND ("diagnosis" OR "evaluation" OR "severity" OR "grading"). Most previous studies on evaluation of meibomian glands (MGs) were relatively subjective and more likely to be affected by interobserver variability, involving invasive operations, and including gland selection errors. It still lacks effective and detailed quantitative analysis tools, and this difficulty poses a challenge for the development of diagnosis, grading, and treatment of meibomian gland dysfunction (MGD).

Added value of this study

Our study developed an automated multiparametric quantitative analyser of MGs in meibography images, and found that increased cross-sectionally uneven gland dilation, decreased gland area ratio, low axial distortion and low signal intensity of MGs showed high risks for the presence of MGD. A combination of all these features has good differentiation power in identifying MGD patients from symptomatic subjects (AUC = 0.82), and the merge of morphological features showed excellent accuracy in distinguishing MGD severities. These variables are quickly assessed by the non-invasive meibography through the self-developed automated algorithm.

Implications of all the available evidence

Since MGD is one of the most common ocular surface diseases degrades patients' quality of life, it often overlaps with dry eye in pathological progress and requires specific meibomian gland-oriented therapies, our automated quantitative analysis of morphological and functional features of MGs have good differentiation power in identifying MGD patients from symptomatic subjects and excellent accuracy in distinguishing MGD severities, which will optimize the clinical management of the disease.

from meibography images have revealed that changes in the secretion and quality of meibum inside meibomian glands could alter the signal intensity of the glands [25]. Exploring the information the signal intensity of MGs in meibography images brings [26] may provide a non-invasive functional indicator to determine whether MGs are in a high- or low-delivery state.

Recently, our team has developed an objective multi-parametric meibomian glands analyser to quantitatively analyse the meibomian glands using infrared meibography images [27]. This analyser can automatically segment and quantitatively analyse the morphological details (gland area ratio, tortuosity, and deformation) and potential functional information from the signal index values of all exposed meibomian glands. The automatic segmentation function of the analyser has been proven to have high similarity compared with manual segmentation by professional ophthalmologists.

The present study aimed to explore the performance of quantitative morphological and functional parameters in meibography images by our self-developed automatic MGs analyser in distinguish MGD patients from people with DED symptoms and MGD grading.

2. Methods

2.1. Data Collection

This cross-sectional, observational study included 256 symptomatic subjects and 56 healthy volunteers. Between January 1, 2019, and December 31, 2020, two-hundred-fifty-six subjects with ocular symptoms related to dry eye disease (DED) were collected from the patient pool of the Zhongshan ophthalmic center (ZOC) Dry Eye Clinic in Guangzhou, China. Fifty-six healthy volunteers without any systemic diseases or pre-existing ocular conditions or symptoms were recruited at the same period from the general population through the ZOC as a normal control group. All participants were required to include information of the Ocular Surface Disease Index (OSDI) symptom questionnaire, ocular surface staining, non-invasive tear-film break-up time (NIBUT), Schirmer I test, meibography, and meibum expressibility and quality. All procedures were conducted following the Declaration of Helsinki (1983) and were approved by the Institutional Review Board of Zhongshan Ophthalmic Centre, Sun Yat-sen University, China (protocol number: 2019KYPJ110). Informed consent was obtained from each of the participants prior to data collection. This study followed STROBE guidelines strictly.

2.2. MGD group and Symptomatic non-MGD group Ascertainment

The diagnosis of MGD was based on an OSDI ≥ 13 and the presence of an altered quality of expressed secretions and/or decreased or absent expression as follows: (1) score >1 for either meibum quality or expressibility or (2) score = 1 for both meibum expressibility and meibum quality [12]. The symptomatic subjects who did not meet the diagnosis criteria mentioned above were defined as symptomatic non-MGD group. One-hundred-ninety-five MGD patients were diagnosed among 256 symptomatic subjects. The remaining 61 subjects without MGs disorders were defined as the symptomatic non-MGD group, including 33 [54.1%] DED cases. Diagnosis of DED in symptomatic non-MGD group was based on NIBUT, Schirmer I test and ocular surface staining: (1) NIBUT < 10 s or (2) Schirmer I test (without anesthesia) ≤ 10 mm in 5min, and a corneal fluorescein staining score of 4 or more based on the corneal staining scale [12]. The MGD patients were further evaluated with regard to the MGD severity level and scored with 1–5 according to the 2011 MGD workshop [12].

2.3. Clinical assessments

The symptom questionnaire OSDI was performed measuring the occurrence frequency of ocular symptoms, environmental triggers

and often overlap in pathological progress [14,15], which leads to the negligence of distinguishing between the two in clinical screening [8]. While MGD requires specific meibomian gland-oriented therapies [16], a non-invasive and objective meibomian gland assessment method to quickly distinguish MGD from people with dry eye symptoms will optimize diagnosis and treatment algorithms.

Noncontact meibography techniques provide ophthalmologists a direct way to visualize the meibomian glands with an inverted eyelid in vivo [17]. Based on meibography images, meibograde was developed as a semiquantitative tool to approximately assess gland loss [17,18], which has been demonstrated to be associated with dry eye [19,20], aging [17], contact lens wearing [3], ocular allergies [21], and severe inflammatory ocular surface diseases [4,5]. Nevertheless, patients with such detectable meibomian gland loss are more likely to be in an advanced stage with seriously impaired meibomian gland function [22]. In fact, detailed morphological features such as gland shortening, distortion, hook, and tortuosity can also be observed in meibography images, some of which are evidence of MGs with worsened expressibility and meibograde [23]. Scholars believe that these gland irregularities may represent an early stage of MGD [9,12,22,24]. Due to the lack of automated quantitative assessment methods, clinical studies on whether and how these diverse detailed morphological features are related to the pathophysiological states of MGD are limited. In addition to morphological changes, observations

and vision related quality of life [28]. Corneal fluorescein staining score is conducted as a standard objective measure to visualize the extent of ocular surface damage [28,29]. Schirmer I test (without anaesthesia) measured the tear secretion to confirm aqueous deficiency [28]. NIBUT and infrared photography of the upper meibomian glands measured by Keratograph 5M (Oculus, Wetzlar, Germany). NIBUT is the interval of time that elapses between a complete blink and the appearance of the first break in the tear film measured by non-invasive methods to evaluate tear film stability [18,28]. Meibum expressibility was scored from the lower central five glands as follows: 0, all five glands; 1, three to four glands; 2, one to two glands; and 3, zero glands [30]. The quality of the expressed meibum was scored from 0-3: 0 = clear fluid; 1 = cloudy fluid; 2 = cloudy, particulate fluid; and 3 = opaque, toothpaste-like meibum [31]. The meibomian gland yield secretion score (MGYSS) was collected from five glands in the central, temporal, and nasal eyelids, for a total of fifteen glands in the lower eyelids. For each of these glands, the secretion was scored as follows: 0: no secretion; 1: inspissated/toothpaste consistency; 2: cloudy liquid secretion; and 3: clear liquid secretion [32]. The scores were then summed across the 15 glands for a single MGYSS, with a range from 0 to 45 [13]. The above assessments were collected from each participant.

One eye was randomly selected for analysis from each non-MGD subject and binocular MGD patient with the same severity. When the severity of MGD was different in both eyes for MGD subjects, the more serious eye was selected.

2.4. Multi-parametric automated meibomian gland analyser

To obtain the quantitative morphological and functional parameters using the acquired infrared meibography images, all images were processed and analysed with our self-developed automated

MGs analyser. For details of the principle and process of this customized software, refer to our previous study [27]. In brief, the meibography images were converted to greyscale, exported and saved as bitmaps, after which they underwent an automated segmentation of the everted tarsal conjunctiva area as the region of interest (ROI), followed by the segmentation and identification of all glands within the ROI (Fig. 1). Then the segmented results were quantitatively analysed with pre-defined morphological and functional parameter calculations, exporting multi-parametric results including the gland area ratio (GA), gland diameter deformation index (DI), gland tortuosity index (TI), and gland signal index (SI). In detail, the gland area ratio is defined as the percentage of detected pixels in the glands over the segmented ROI area; the gland diameter DI addresses the diameter variations of a gland, such as uneven dilation and discontinuous atrophy; the gland TI is used to quantify the degree of curving and hair-pin-loop-like winding changes of the glands; and the gland SI is the average image greyscale value of the segmented intact glands divided by the average image greyscale value of the non-gland area.

2.5. Statistical analysis

Comparisons of measurements among the three groups were assessed by analysis of variance (ANOVA) for normally distributed continuous variables and chi-squared test for categorical variables. The SI was transformed into categorical variables corresponded to clinical observation of the low, moderate, and high signal intensity of glands as low-level SI ($SI < 4.5$), medium-level SI ($4.5 \leq SI \leq 6.5$) and high-level SI ($SI > 6.5$). The cut-off values were set between two subgroups (10 cases as a unit) with large differences in prevalence of MGD in ascending range of SI. Bivariate correlations were performed using Spearman correlations coefficients between multiple measurements of MGs and MGYSS in all subjects with completed ocular

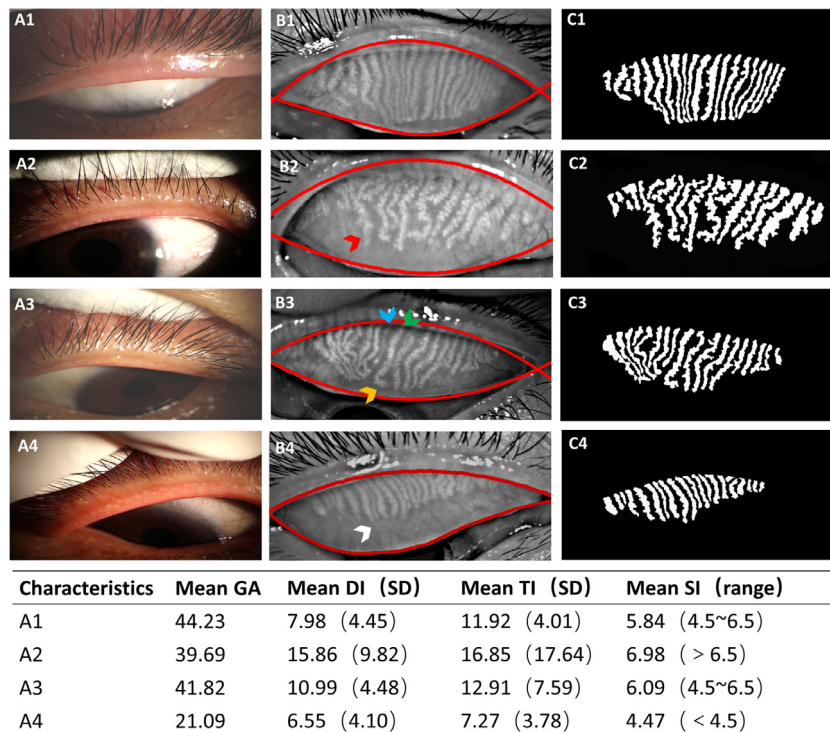


Fig. 1. (A) the appearance of the lid margins and meibomian orifices, (B) the Meibography images with automatically segmented boundaries of the everted tarsal conjunctiva area as the region of interest (ROI), and (C) the segmented meibomian glands of representative subjects. The sequence from 1 to 4 is based on the current stage of MGs pathological progression from healthy to severe. Examples of the targeted individual features of tortuosity (yellow arrow), dilation & distortion (red arrow), and ghost glands with a declined signal index (blue arrow), an increased signal index (green arrow), and atrophy or drop out (white arrow) are marked with arrows. The acquired multi-parametric analysis results of the four representative Meibography images are shown in the table below the figure. DI: diameter deformation index; TI: tortuosity index SI: signal index; SD: standard deviation; GA: gland area ratio, which is the ratio of all meibomian gland area to the total analysis area.

surface examination mentioned above ($n = 312$). Binary logistic regression was conducted to identify the independent correlations of multiple measurements of MGs associated with MGD diagnosis. Variables were considered for adjustment in the binary logistic regression model if they displayed a P value of less than 0.05 in the tests of between-group comparison. Sex and age were also considered for adjustment in the model.

By dividing all the symptomatic subjects ($n = 256$) into a training set and a test set with a ratio of 80%: 20%, the detection probability of the multiple measurements of MGs to discriminate MGD from symptomatic subjects was evaluated by performing regression model with the training set and calculating the area under the curve of a receiver operating characteristic curve (AUC-ROC) in the test set. Kendall's tau-b correlation was performed in symptomatic subjects between multiple measurements of MGs and severities to screen potential grading indicators. The prediction value of each potential grading indicator for each grade (grade 1–5) was evaluated with AUC-ROCs. The grading performance of the combined features were also evaluate by testing AUC-ROCs from training regression models by subdividing each grade into training and test sets (80%: 20%). The statistical analyses above were performed in SPSS 20.0 (SPSS, Chicago, IL). $P < 0.05$ were considered statistically significant. P -values were adjusted by Bonferroni correction in multiple comparisons.

2.6. Role of funding sources

All sources of funding had no role in study design, data collection, data analysis, data interpretation or writing of this manuscript, or the decision to submit it for publication. The corresponding authors had

full access to all the data in the study and had final responsibility for the decision to submit for publication.

3. Results

3.1. The clinical measurements, morphological and functional analysis of MGs among groups

Typical cases with the appearance of lid margins, segmented meibomian glands, and the acquired multi-parametric analysis results of the glands are shown in Fig. 1. Data for the clinical measurements, the morphological and functional measurements of MGs of all eligible participants ($n = 312$) from the MGD group ($n = 195$), symptomatic non-MGD group ($n = 61$) and normal group ($n = 56$) and the P values from pairwise comparisons of the values among the 3 groups are presented in tables 1 and 2, respectively. Age and sex showed no significant difference within each pair of subject groups. Adverse changes in the OSDI, NI-BUT, meibum expressibility, MGYSS, corneal fluorescein staining (CFS) score, and Schirmer's I test were increased significantly in the MGD group compared to the normal group and the symptomatic non-MGD group. The GA (41.07%) and TI (13.44) were found in the MGD group lower than in the symptomatic non-MGD group (GA 47.74%, TI 14.90) and normal group (GA 47.25%, TI 14.66) ($P < 0.05$, respectively). The DI was 12.84 in the MGD group, significantly higher than in the symptomatic non-MGD group (DI 9.62) and normal group (DI 10.83) ($P < 0.05$, respectively). The normal group showed the highest frequency of a medium-level SI (76.79%). The MGD groups showed the highest frequency of both a low-level SI (25.13%) and a high-level-SI (26.15%) among three groups. (tables 1 and 2).

Table 1
Clinical parameters and morphological & functional parameters of MGs for the 3 groups of study subjects

Parameter	Symptomatic groups		Normal Control	P of trend value
	MGD	Symptomatic non-MGD		
No. of subjects	195	61	56	
Age, mean (SD), yrs	34.47 (11.53)	33.50 (12.36)	31.65 (9.38)	0.26
Sex, no. (%)				0.15
Female	118 (60.51)	33 (54.09)	40 (71.43)	
Male	77 (39.49)	28 (45.91)	16 (28.57)	
Severity, no. (%)				<0.001
Grade 0	0	61 (100)	56 (100)	
Grade 1	47 (24.10)	0	0	
Grade 2	64 (32.82)	0	0	
Grade 3	47 (24.10)	0	0	
Grade 4	28 (14.36)	0	0	
Grade 5	9 (4.62)	0	0	
Expressibility, no. (%)				<0.001
0	9 (4.62)	51 (83.61)	44 (78.57)	
1	89 (45.64)	10 (16.39)	12 (21.43)	
2	63 (32.31)	0	0	
3	34 (17.44)	0	0	
OSDI, mean (SD)	25.87 (10.56)	17.05 (6.55)	3.89 (2.77)	<0.001
NI-BUT, mean (SD), s	8.80 (4.81)	12.95 (5.14)	16.25 (4.92)	<0.001
MGYSS, mean (SD)	24.18 (7.12)	40.54 (6.30)	41.59 (3.93)	<0.001
CFS score, mean (SD)	0.87 (0.88)	0.05 (0.22)	0.00	<0.001
ST I, mean (SD), mm	12.25 (6.24)	16.48 (6.05)	16.39 (6.65)	<0.001
Morphological parameters				
DI, mean (SD)	12.84 (5.77)	9.62 (2.76)	10.83 (2.87)	<0.001
TI, mean (SD)	13.44 (2.77)	14.90 (3.22)	14.66 (2.46)	<0.001
GA, mean (SD), %	41.07 (10.22)	47.74 (6.67)	47.25 (8.16)	<0.001
Functional parameter:SI range, no (%)				
SI<4.5	49 (25.13)	6 (9.84)	3 (5.36)	
4.5≤SI≤6.5	95 (48.72)	42 (68.85)	43 (76.79)	
SI>6.5	51 (26.15)	13 (21.31)	10 (17.86)	

Abbreviations: MGs: meibomian glands; MGD: meibomian gland dysfunction; SD: standard deviation; OSDI: ocular surface disease index; NI-BUT: non-invasive tear film break-up; MGYSS: meibomian gland yield secretion score; CFS: corneal fluorescein staining score; ST I: Schirmer test I; DI: diameter deformation index; TI: tortuosity index; GA: gland area ratio, which is the ratio of all meibomian gland area to the total analysis area; SI: signal index of the glands.

Table 2

P Values for statistical comparison of clinical parameters and morphological & functional measurements of MGs among groups

Parameter	MGD vs. Symptomatic non-MGD	MGD vs. Normal Control	Symptomatic non-MGD vs. Normal Control
OSDI	<0.001	<0.001	<0.001
NI-BUT (s)	<0.001	<0.001	0.001
Meibum expressibility (0-3)	<0.001	<0.001	>0.99
MGYSS	<0.001	<0.001	>0.99
CFS score	<0.001	<0.001	>0.99
ST I (mm)	0.04	<0.001	0.49
Morphological parameters			
DI	<0.001	0.02	0.54
TI	0.001	0.01	>0.99
GA (%)	<0.001	<0.001	>0.99
Functional parameter: SI range	0.01	<0.001	0.55

Abbreviations: MGs: meibomian glands; MGD: meibomian gland dysfunction; SD: standard deviation; OSDI: ocular surface disease index; NI-BUT: non-invasive tear film break-up; MGYSS: meibomian gland yield secretion score; CFS: corneal fluorescein staining score; ST I: Schirmer test I; DI: diameter deformation index; TI: tortuosity index; GA: gland area ratio; SI: signal index of the glands.

3.2. Evaluation of the diagnosis performance of the multiple measurements of MGs in MGD

Table 3 demonstrates results from the binary logistic regression models concerning how the DI, TI, GA, and SI of MGs discriminated MGD from symptomatic non-MGD subjects (n = 256), controlling for age, sex, MGYSS, NIBUT, FSC score and Schirmer test I. With the results reported as estimated odds ratios (95% CI), the increase of the DI (1.62 [1.29-2.56]) and the number of subjects with an SI under 4.5 (24.34 [2.73-217.30]) demonstrated significant positive associations with the presence of MGD. An increased TI (0.76 [0.54-0.90]) and GA (0.86 [0.74-0.92]) showed negative associations with the presence of MGD. The accuracy of identifying whether a symptomatic individual had MGD based on the DI, TI, GA, and SI was evaluated to calculate the AUC-ROC and showed that AUC = 0.82 (P < 0.001) in the test set (Fig. 2).

3.3. Evaluation of the clinical associations and grading performances of multiple measurements of MGs

Significant associations were found between the MG morphological parameters (DI, TI, and GA) and MGYSS (all P < 0.05, Fig. 3). The Spearman coefficients for the correlations between morphological parameters (GA, TI, and DI) and MGYSS were 0.40, 0.22 and -0.19. In symptomatic subjects, the DI, TI and GA were significantly associated with MGD severities, Kendall's tau-b correlation coefficients were 0.15 (P = 0.001), -0.25 (P < 0.001), and -0.40 (P < 0.001), respectively, excluding the SI (P = 0.25). The ROC curve analysis for the single and combined morphological parameter with respect to each level of MGD severity can also be seen in table 4. The performance of single variables showed that DI had a highest AUC-ROC in identifying early-stage MGD (grade 1, 0.76, P < 0.001; grade 2, 0.74, P < 0.001). GA had highest AUC-ROCs in moderate and advanced stages (grade 3, 0.83, P < 0.001; grade 4, 0.92, P < 0.001; grade 5, 1.00, P < 0.001), followed by TI (grade 3, 0.70, P = 0.001; grade 4, 0.77, P < 0.001; grade 5, 0.92,

P < 0.001). The combined DI-TI-GA showed the highest AUC-ROCs compared to single variables in each grade in the test sets (grade 1, 0.79, P = 0.03; grade 2, 0.80, P = 0.01; grade 3, 0.87, P = 0.004; grade 4, 0.94, P = 0.003; grade 5, 1.00, P = 0.03) (table 4). The specific trends of the 3 morphological parameters across different severities can be visualized in figure 4.

4. Discussion

In the present study, we reported a comprehensive analysis of MGs based on an automated algorithm [27] using meibography images by quantifying the gland area ratio as GA, the gland irregular shapes as DI and axial distortions as TI in morphological analysis. Quantification of the optical density of the glands relative to the background as the SI produced a potential functional index of MGs. Our results demonstrated that the multi-measurements of MGs (DI, TI, GA and SI) from the regression model adjustment for sex, age and other pathologic changes on the ocular surface that may affect the presentation of disease [17,33] were associated significantly with the presence of MGD. The combination of DI-TI-GA-SI showed an excellent diagnosis performance in identification of MGD patients from people with suspected DED, which will benefit to fast screen for MGD in symptomatic population. The assessments of the morphological multi-parameters of MGs (DI, TI, and GA) have good consistency with the evaluation of meibum quality and expressibility (MGYSS), reflected typical objective changes in different MGD pathological stages. Merging the morphological parameters (DI-TI-GA) could

Table 3

Variables in the equation of the binary regression

	P value	OR#	95% CI	
			Lower	Upper
DI	0.001	1.62	1.29	2.56
TI	0.006	0.76	0.54	0.90
GA (%)	0.001	0.86	0.74	0.92
SI < 4.5 vs. 4.5 ≤ SI ≤ 6.5	0.004	24.34	2.73	217.30
SI > 6.5 vs. 4.5 ≤ SI ≤ 6.5	0.96	0.96	0.19	4.80

#: OR adjusted for sex, age, MGYSS, NIBUT, CFS score and Schirmer test I.

Abbreviations: DI: diameter deformation index; TI: tortuosity index; GA: gland area ratio; SI: signal index of the glands.

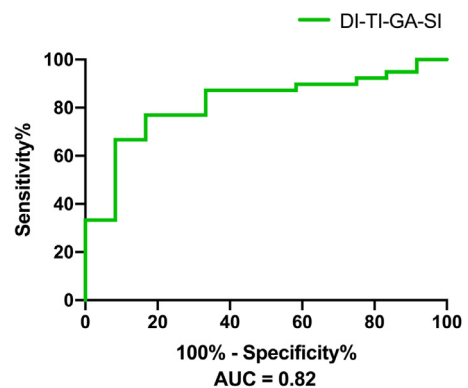


Fig. 2. The ROC curves of the combination of morphological parameters for MGD diagnosis from the test set. Patients were diagnosed based on an altered quality of expressed secretions and/or decreased or absent expression, with the presence of ocular symptoms. The area under the ROC curve (AUC) for the combination of the DI, TI, GA (%) and SI to discriminate MGD from symptomatic non-MGD patients was 0.82. ROC: receiver operating characteristic. DI: diameter deformation index. TI: tortuosity index. GA: gland area ratio, which is the ratio of all meibomian gland area to the total analysis area. SI: signal index of the glands.

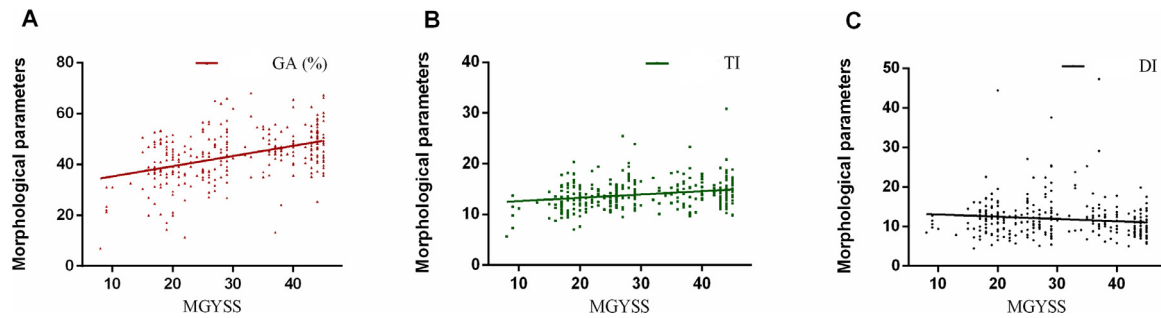


Fig. 3. Scatterplots for the correlations between average morphological parameters of MGs and MGYS. The GA (%), TI, and DI were significantly correlated with MGYS ($P < 0.001$). The Spearman coefficients were r_{GA} : 0.40, r_{TI} : 0.22 and r_{DI} : -0.19. MGYS: meibomian gland yield secretion score, DI: diameter deformation index; TI: tortuosity index; GA: gland area ratio, the ratio of all meibomian gland area to total analysis area.

complement each other to increase the accuracy of to distinguish MGD severities. The automatic quantitative multi-measurements of detailed morphological and functional information from meibography images provide a non-invasive, fast, and easy processing method for MGD diagnosis and grading.

The GA was calculated as the whole MGs area ratio by eliminating the gaps between glands, which can reflect additional information of gland thickening, thinning and abnormal gaps compared to MGs drop out quantified as meibograde [22,34]. The thinned glands and large gaps had been observed and determined to represent incomplete gland atrophy in the DREAM study [35]. While MGs drop out was reported to represent the final stage of MGD [22], our study demonstrated that a decreased GA was independently associated with the presence of MGD from level 2 to level 5, revealed a thinned glands and large gaps were also involved in the progression of the disease. Conversely, for the lowest MGD severity (level 1), the GA was slightly increased, which may be a result of MG dilation and thickening. Increased MGs thickness was also observed to be inversely correlated with meibum expression and considered to be a compensatory response to gland loss and increased meibum demand [36]. Dilation of secretory acini could be part of the same process, as a result of the expansion of accumulated and inspissated debris within the acini observed in previous studies [23,37,38].

A typical dilation pattern was proven by another morphological parameter—the diameter deformation index (DI), which addresses the degree of diameter variations to present the uneven thickening or thinning of MGs. A high DI was observed in the MGs of early pathological stages (level 1-3) and declined at levels 4 and 5. ROC-AUCs analysis also showed that the DI had better predictive accuracy in the earliest stage, indicating that the increased DI may be a sensitive marker of early MGD before visible glands loss. These findings are consistent with previous objective observations that gland dilation is an early visual pathogenic finding and associated with progressive loss of MGs [22]. The pattern of uneven thickening or thinning can result from progressive pressure due to partial obstruction of the

ductal system and an inflammatory process of the secretory acinus [22,39].

It has been confirmed that curving and hairpin-loop-like tortuosity as another morphology pattern occur both in progressive distortion of the ductal system [39,40] and asymptomatic people [41]. Whether the tortuosity of MGs could translate into a pathological change [42] or only a congenital pattern [41] is still controversial. In this study, the TI showed no significant change compared to symptomatic non-MGD and normal group in the early stage of MGD (level 1-2) but showed similarities with the GA that decreased significantly in moderate and severe MGD with increased severities prediction accuracy. Therefore, axial distortion is more likely to be a kind of congenital morphology pattern and not sensitive enough to be used as a single indicator for MGD diagnosis in the early stage, and a decline TI with a reduction of the GA can represent overall gland atrophy, which is different from gland dropout or shortened glands, as a complement sign of severe loss of acinar cells in late pathological stages.

Existing functional examinations of the MGs such as the meibum quality and expressibility, which have limitations of only assessing several glands and are impossible to conduct when the gland is completely obstructed. Since changes in the consistency and colour of the meibum have been observed under pathological conditions [39], we defined the gland signal index (SI) to provide a non-contact biomarker that may offer functional information by quantifying the optical density of the meibum within the ductal system. We demonstrated that subjects with an extreme SI, who were defined as those with low levels (< 4.5) and high levels (> 6.5), were found to

Table 4

Receiver operating characteristic curve analysis for the combination and each morphological parameter with respect to each grade of MGD severity

Severities	DI		TI		GA (%)		DI-TI-GA	
	AUC	P	AUC	P	AUC	P	AUC	P
Grade 1	0.76*	<0.001	0.57	0.19	0.52	0.73	0.79*	0.03
Grade 2	0.74*	<0.001	0.60*	0.04	0.67*	0.001	0.80*	0.01
Grade 3	0.67*	0.003	0.70*	0.001	0.83*	<0.001	0.87*	0.004
Grade 4	0.68	0.08	0.77*	<0.001	0.92*	<0.001	0.94*	0.003
Grade 5	0.68	0.08	0.90*	<0.001	1.00*	<0.001	1.00*	0.03

*: P value <0.05.

Abbreviations: MGD: meibomian gland dysfunction; DI: diameter deformation index; TI: tortuosity index; GA: gland area ratio.

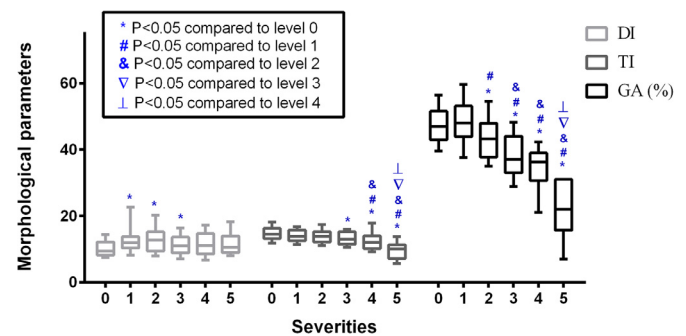


Fig. 4. Boxplots for the comparison of morphological parameters across different severity levels. The DI, TI, and GA (%) across levels 0~5 of MGD severity are shown. Significant increases in the DI are shown at levels 1~3, while significant decreasing trends are shown in the TI at levels 3~5. The GA (%) increased slightly at level 1 and then gradually decreased at levels 2~5. In all box plots, boxes represent the interquartile ranges (IQRs) between the first and third quartiles, and the line inside the box represents the median; whiskers represent the lowest or highest values within 1.5 times IQR from the first or third quartiles. Different symbols indicate significant differences compared to different groups. DI: diameter deformation index; TI: tortuosity index; GA: gland area ratio, which is the ratio of all meibomian gland area to the total analysis area.

constitute a higher proportion of the MGD group than the symptomatic non-MGD group and normal group. Moreover, low-level SI MGs harbour a 24.3-fold increased adjusted risk for the presence of MGD compared to patients with a medium-level SI (4.5~6.5) of MGs (OR: 24.34, 95% CI 2.73 – 217.30). Although the large confidence interval indicate sort of uncertainty, potentially due to the large dispersion of SI itself and the conversion of continuous SI values into categorical variables, the large impact of the low-level SI in MGD deserves clinical attention. The low-level SI represents dim glands with low optical signals, which is in agreement with the study by Daniel et al [35], who observed a large number of pale glands were associated with eyelids expressed none or thick paste like consistency sebum. We concluded that the low-level SI MGs are sick glands with low-delivery state progressing towards atrophy. The high-level SI could be related to the excessive accumulation of meibum in MGs caused by obstruction or typical lipid compositions [43]. Thus, SI may provide an overall assessment of glands function to assist MGD classification.

In this study, only the upper eyelids were included since the upper lids were demonstrated to have more visible MG features and a stronger correlation with clinical signs than lower lids [35]. Moreover, meibography images of the lower eyelid are more likely to show unevenly focused and uncompleted exposed meibomian glands, which are challenging in automatic segmentation and analysis. To further clarify the clinical potential and pathologic information provided by morphological and functional measurements of MGs, a prospective cohort study to track longitudinal changes in meibomian glands from disease or intervention will also be necessary in the future. In addition to DED and MGD, the morphology and function of MGs are also observed to related to many ocular and systemic abnormalities, i.e., allergic conjunctivitis, ocular rosacea, dyslipidemia, diabetes, and aging, etc. [3-5,6-8,17], the automatic and quantitative methods established in this study could have extended application prospects in future studies regarding the roles of MGs in other related ocular and systematic conditions.

In conclusion, with the automated multiparametric quantitative analysis of MGs in meibography images, our study found that morphological features including an increased DI (cross-sectionally uneven gland dilation) and a slightly increased GA (thickened and dilated glands) are common in the early stage of MGD, while a decreased GA (greatly influenced by incomplete atrophy) together with a decreased TI (decreased axial distortion) are signs of severe MGD, and revealed that glands with a low-level SI showed a high risk for the presence of MGD. A combination of DI-TI-GA-SI has good differentiation power in identifying MGD patients from symptomatic subjects, and the merge of morphological parameters DI-TI-GA showed excellent accuracy in distinguishing MGD severities.

Funding

This work was supported by the Key-Area Research and Development Program of Guangdong Province (No. 2019B010152001), the National Natural Science Foundation of China under Grant (81901788) and Guangzhou Science and Technology Program (202002030412).

Contributors

JY and PX devised the project, the main conceptual ideas and proof outline. YQ-D contributed to the design and implementation of the research and the analysis of the results and to the writing of the manuscript. QW supervised the findings of this work and contributed to the writing of the manuscript. ZZ-L & PX developed and verified the automatic Meibomian glands analyser, and aided in interpreting the results and worked on the manuscript. SQ-L, JZ, BW-W, and LL-P performed the measurements and performed the analysis of data. All authors discussed the results and commented on the manuscript. JY,

PX and YQ-D accessed and were responsible for the raw data associated with the study.

Data sharing statement

All data will be available upon reasonable request to the corresponding author, and it will be shared according to the standards of ethical policies regulating data sharing of human subjects.

Declaration of Competing Interest

We declare no conflicts of interests.

Acknowledgements

Additional assistance in the conduct of this study was provided by Ke Ma BSC, HongLiang Xue PhD, Ziqing Feng MD.

References

- [1] Schaumberg DA, Nichols JJ, Papas EB, Tong L, Uchino M, Nichols KK. The international workshop on meibomian gland dysfunction: report of the subcommittee on the epidemiology of, and associated risk factors for, MGD. *Invest Ophthalmol Vis Sci* 2011;52:1994-2005.
- [2] Stapleton F, Alves M, Bunya VY, et al. TFOS DEWS II Epidemiology Report. *Ocul Surf* 2017;15:334-65.
- [3] Llorens-Quintana C, Garaszczuk IK, Szczesna-Iskander DH. Meibomian glands structure in daily disposable soft contact lens wearers: a one-year follow-up study. *Ophthalmic Physiol Opt* 2020;40:607-16.
- [4] Sullivan DA, Dana R, Sullivan RM, et al. Meibomian Gland Dysfunction in Primary and Secondary Sjogren Syndrome. *Ophthalmic Res* 2018;59:193-205.
- [5] Lekhanont K, Jongkhajornpong P, Sontichai V, Anothaisintawee T, Nijvipakul S. Evaluating Dry Eye and Meibomian Gland Dysfunction With Meibography in Patients With Stevens-Johnson Syndrome. *Cornea* 2019;38:1489-94.
- [6] Wang MTM, Vidal-Rohr M, Muntz A, et al. Systemic risk factors of dry eye disease subtypes: A New Zealand cross-sectional study. *Ocul Surf* 2020;18:374-80.
- [7] Sandra Johanna GP, Antonio LA, Andres GS. Correlation between type 2 diabetes, dry eye and Meibomian glands dysfunction. *J Optom* 2019;12:256-62.
- [8] Arita R, Mizoguchi T, Kawashima M, et al. Meibomian Gland Dysfunction and Dry Eye Are Similar but Different Based on a Population-Based Study: The Hirado-Takushima Study in Japan. *Am J Ophthalmol* 2019;207:410-8.
- [9] Nelson JD, Shimazaki J, Benitez-del-Castillo JM, et al. The international workshop on meibomian gland dysfunction: report of the definition and classification subcommittee. *Invest Ophthalmol Vis Sci* 2011;52:1930-7.
- [10] Qiao J, Yan X. Emerging treatment options for meibomian gland dysfunction. *Clin Ophthalmol* 2013;7:1797-803.
- [11] Bron AJ, Tiffany JM. The contribution of meibomian disease to dry eye. *Ocul Surf* 2004;2:149-65.
- [12] Tomlinson A, Bron AJ, Korb DR, et al. The international workshop on meibomian gland dysfunction: report of the diagnosis subcommittee. *Invest Ophthalmol Vis Sci* 2011;52:2006-49.
- [13] Lane SS, DuBiner HB, Epstein RJ, et al. A new system, the LipiFlow, for the treatment of meibomian gland dysfunction. *Cornea* 2012;31:396-404.
- [14] Chan TCY, Chow SSW, Wan KHN, Yuen HKL. Update on the association between dry eye disease and meibomian gland dysfunction. *Hong Kong Med J* 2019;25:38-47.
- [15] Milner MS, Beckman KA, Luchs JI, et al. Dysfunctional tear syndrome: dry eye disease and associated tear film disorders - new strategies for diagnosis and treatment. *Curr Opin Ophthalmol* 2017;27 Suppl 1:3-47.
- [16] Baudouin C, Messmer EM, Aragona P, et al. Revisiting the vicious circle of dry eye disease: a focus on the pathophysiology of meibomian gland dysfunction. *Br J Ophthalmol* 2016;100:300-6.
- [17] Arita R, Itoh K, Inoue K, Amano S. Noncontact infrared meibography to document age-related changes of the meibomian glands in a normal population. *Ophthalmology* 2008;115:911-5.
- [18] de Paiva CS, Lindsey JL, Pflugfelder SC. Assessing the severity of keratitis sicca with videokeratographic indices. *Ophthalmology* 2003;110:1102-9.
- [19] Arita R, Itoh K, Maeda S, et al. Proposed diagnostic criteria for obstructive meibomian gland dysfunction. *Ophthalmology* 2009;116:2058-63.
- [20] Pflugfelder SC, Tseng SC, Sanabria O, et al. Evaluation of subjective assessments and objective diagnostic tests for diagnosing tear-film disorders known to cause ocular irritation. *Cornea* 1998;17:38-56.
- [21] Ibrahim OM, Matsumoto Y, Dogru M, et al. In vivo confocal microscopy evaluation of meibomian gland dysfunction in atopic-keratoconjunctivitis patients. *Ophthalmology* 2012;119:1961-8.
- [22] Xiao J, Adil MY, Olafsson J, et al. Diagnostic Test Efficacy of Meibomian Gland Morphology and Function. *Sci Rep* 2019;9:17345.
- [23] Srinivasan S, Menzies K, Sorbara L, Jones L. Infrared imaging of meibomian gland structure using a novel keratograph. *Optom Vis Sci* 2012;89:788-94.

- [24] Knop E, Knop N, Brewitt H, et al. [Meibomian glands: part III. Dysfunction - argument for a discrete disease entity and as an important cause of dry eye]. *Ophthalmologie* 2009;106:966–79.
- [25] Yeh TN, Lin MC. Repeatability of Meibomian Gland Contrast, a Potential Indicator of Meibomian Gland Function. *Cornea* 2019;38:256–61.
- [26] Blackie CA, Korb DR. The diurnal secretory characteristics of individual meibomian glands. *Cornea* 2010;29:34–8.
- [27] Peng Xiao, Zhongzhou Luo, Yuqing Deng. An automated and multi-parametric algorithm for objective analysis of meibography images. *Quantitative Imaging in Medicine and Surgery* 2021;11:1586–99.
- [28] Wolffsohn JS, Arita R, Chalmers R, et al. TFOS DEWS II Diagnostic Methodology report. *Ocul Surf*. 2017;15(3):539–74.
- [29] Lemp MA. Report of the National Eye Institute/Industry workshop on Clinical Trials in Dry Eyes. *CLAO J* 1995;21:221–32.
- [30] Bron AJ, Benjamin L, Snibson GR. Meibomian gland disease. Classification and grading of lid changes. *Eye (Lond)* 1991;5(Pt 4):395–411.
- [31] Yin Y, Gong L. The evaluation of meibomian gland function, morphology and related medical history in Asian adult blepharokeratoconjunctivitis patients. *Acta Ophthalmol* 2017;95:634–8.
- [32] Golebiowski B, Chim K, So J, Jalbert I. Lid margins: sensitivity, staining, meibomian gland dysfunction, and symptoms. *Optom Vis Sci* 2012;89:1443–9.
- [33] Nien CJ, Paugh JR, Massei S, Wahlert AJ, Kao WW, Jester JV. Age-related changes in the meibomian gland. *Exp Eye Res* 2009;89:1021–7.
- [34] Villani E, Arita R. Imaging of meibomian glands: from bench to bedside and back. *Eye (Lond)* 2019;33:695–7.
- [35] Daniel E, Maguire MC, Pistilli M, et al. Grading and baseline characteristics of meibomian glands in meibography images and their clinical associations in the Dry Eye Assessment and Management (DREAM) study. *Ocul Surf* 2019;17:491–501.
- [36] Villani E, Marelli L, Dellavalle A, Serafino M, Nucci P. Latest evidences on meibomian gland dysfunction diagnosis and management. *Ocul Surf* 2020;18:871–92.
- [37] Koh YW, Celik T, Lee HK, Petznick A, Tong L. Detection of meibomian glands and classification of meibography images. *J Biomed Opt* 2012;17:086008.
- [38] Matsumoto Y, Sato EA, Ibrahim OM, Dogru M, Tsubota K. The application of in vivo laser confocal microscopy to the diagnosis and evaluation of meibomian gland dysfunction. *Mol Vis* 2008;14:1263–71.
- [39] Knop E, Knop N, Millar T, Obata H, Sullivan DA. The international workshop on meibomian gland dysfunction: report of the subcommittee on anatomy, physiology, and pathophysiology of the meibomian gland. *Invest Ophthalmol Vis Sci* 2011;52:1938–78.
- [40] Fuchs E. Scratching the surface of skin development. *Nature* 2007;445:834–42.
- [41] Zhao Y, Chen S, Wang S, et al. The significance of meibomian gland changes in asymptomatic children. *Ocul Surf* 2018;16:301–5.
- [42] Wang MTM, Craig JP. Natural history of dry eye disease: Perspectives from inter-ethnic comparison studies. *Ocul Surf* 2019;17:424–33.
- [43] Dougherty JM, McCulley JP. Bacterial lipases and chronic blepharitis. *Invest Ophthalmol Vis Sci* 1986;27:486–91.